PHYSICAL REVIEW B **80**, 060504(R) (2009)

Limits on Bose-Einstein condensation in confined solid ^{4}He

S. O. Diallo,[1,2] R. T. Azuah,[3,4] O. Kirichek,[5] J. W. Taylor,[5] and H. R. Glyde[1]
[1]*Department of Physics and Astronomy, University of Delaware, Newark, Delaware 19716-2593, USA*
[2]*Ames Laboratory, U.S. DOE, Ames, Iowa 50011, USA*
[3]*NIST Center for Neutron Research, Gaithersburg, Maryland 20899-8562, USA*
[4]*Department of Materials Science and Engineering, University of Maryland, College Park, Maryland 20742-2115, USA*
[5]*ISIS Spallation Neutron Source, Rutherford Appleton Laboratory, Chilton, Didcot OX11 0QX, United Kingdom*
(Received 15 July 2009; published 12 August 2009)

We report neutron-scattering measurements of the Bose-Einstein condensate (BEC) fraction, n_0, in solid helium that has a large surface to volume (S/V) ratio. Rittner and Reppy observed large superfluid fractions, ρ_S/ρ, in large S/V samples with ρ_S/ρ approximately proportional to S/V, up to $\rho_S/\rho=20\%$ at $S/V=150$ cm^{-1}. Our goal is to reveal whether there is BEC associated with these large ρ_S/ρ. Our solid volume is 100 cm^3 of commercial grade helium at 41 bars pressure ($T_c\simeq 200$ mK) in a cell that has $S/V=40$ cm^{-1} that cannot be quenched rapidly. We find no evidence for BEC or algebraic off diagonal long-range order with $n_0=0.0\pm 0.3\%$ at 65 mK.

DOI: 10.1103/PhysRevB.80.060504 PACS number(s): 67.80.bd, 78.70.Nx, 67.85.Hj

In 2004, Kim and Chan[1,2] reported that below a critical temperature $T_c\simeq 200$ mK a fraction of solid helium ceased to oscillate in torsional oscillator (TO) measurements. This nonclassical rotational inertia (NCRI) below T_c has been interpreted as a signature of supersolid behavior—remarkably extending superflow to solids.

An NCRI in TOs below T_c and its temperature dependence below T_c has since been confirmed in several laboratories[3–6] and is now well established. However, the magnitude of the superfluid fraction, ρ_S/ρ, reported varies dramatically, from 0.015% to 20%, depending on the experimental conditions such as how the solid is prepared and cooled, on subsequent annealing, on the sample geometry, on the ^{3}He concentration, and on other factors.[7–9] This suggests that the NCRI is associated with defects such as dislocations, grain boundaries, point defects, glassy regions, or surfaces. This association with defects is supported by Monte Carlo calculations, which find that in perfect crystals of solid helium both the ρ_S/ρ and the Bose-Einstein condensation (BEC) fraction, n_0, are unobservably small.[10–12] However, observable values of ρ_S/ρ and condensate fractions $n_0\simeq 0.3-0.5\%$ have been calculated for glassy (amorphous) solid helium[11] and in solid helium containing vacancies.[13,14] Amorphous regions in bulk solid helium[15] and completely amorphous solid helium in porous media[16] have now been observed. Particularly intriguing, Rittner and Reppy[17] found large superfluid fractions in solid samples that have a large surface area to volume ratio (S/V)—with ρ_S/ρ approximately proportional to S/V and reaching 20% at $S/V=150$ cm^{-1}. These large ρ_S/ρ values are not universally observed and may arise from rapid cooling of thin samples.[18]

Surprisingly, the sheer modulus (μ) of solid helium shows[19] an unexpected increase below T_c. The increases in μ and in ρ_S/ρ have the same dependence on temperature and ^{3}He concentration suggesting a common physical origin. However, recent measurements[20] show that μ increases in hcp crystals only (both ^{4}He and ^{3}He) while an NCRI is observed in ^{4}He only, both bcc and hcp. An unexplained contribution to the heat capacity[21,22] that peaks at T_c and bulk mass flow in solids near the melting line[23,24] has been reported. For reviews see Refs 14 and 25–27.

The observation of BEC below T_c would be an unambiguous verification that the observed NCRI indeed arises from superflow. In bulk three-dimensional (3D) systems, superflow is a consequence of BEC.[28] In two-dimensional (2D) bulk systems, the onset of superflow[29] is associated with the onset of order[30,31] that can be observed[32] in a similar way as BEC. In finite-sized systems superflow is also associated with BEC, and in all three cases there is a peaking of the atomic momentum distribution $n(\mathbf{k})$ at $\mathbf{k}=0$ below T_c. The goal of the present measurements is to search for BEC. We use a sample that has $S/V=40$ cm^{-1}, where large values of ρ_S/ρ have been observed, and commercial grade helium (^{3}He concentration 0.3 ppm) where $T_c\simeq 200$ mK. The cell volume is large, 100 cm^3. While this improves the statistical precision by a factor of 5 beyond our previous measurements,[33] it means we cannot cool the solid rapidly. We observe no changes in $n(\mathbf{k})$ above and below T_c within precision. This may be expressed as a BEC fraction $n_0=0.0\pm 0.3\%$ at 65 mK. In commercial grade helium, the observed NCRI saturates to its maximum value at $T=50$ mK. Thus we have not observed BEC and are not able to confirm that NCRI below T_c is superflow at this time.

The solid helium sample cell is shown in Fig. 1. The cell contained 95 parallel aluminum sheets of thickness 0.05 mm. There was a well-defined spacing $d=0.5$ mm filled with helium between each sheet so that $S/V=2/d=40$ cm^{-1}. The neutron beam entered the cell parallel to the aluminum sheets.

The solid was grown from liquid in the cell using the blocked capillary method. The capillary blocked at an initial pressure of 70 bars and the final pressure was 41 bars corresponding to complete solidification to an hcp solid at $V_m=19.8$ cm^3/mol. Three hcp Bragg peaks were observed that confirmed this solid volume.

The neutron-scattering measurements were carried out on the MARI time of flight (TOF) spectrometer at the ISIS Facility, Rutherford Appleton Laboratory, U.K. The TOF data

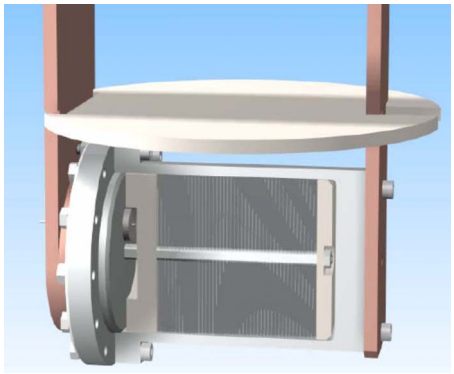

FIG. 1. (Color online) Sample cell of diameter 50 mm and length 55 mm containing 100 cm^3 of solid helium. The cell contains 95 parallel aluminum sheets separated a distance $d=0.5$ mm giving a sample surface to volume ratio $(S/V)=2/d=40$ cm^{-1}.

were converted to the dynamic structure factor $J(Q,y)$ at constant wave-vector transfer Q in the range $20 \leq Q \leq 29$ $Å^{-1}$ and energy transfer $(\hbar\omega)$ expressed in the y variable, $y=(\omega-\omega_R)/(\hbar Q/m)$ where $\omega_R=(\hbar Q^2/2m)$.

To analyze the data, we introduce a model atomic momentum distribution,

$$n(\mathbf{k}) = n_0\delta(\mathbf{k}) + (1-n_0)n^*(\mathbf{k}), \tag{1}$$

where n_0 is the condensate fraction and $n^*(\mathbf{k})$ is the distribution over states above the condensate. Equation (1) assumes no coupling between the $k=0$ and $k>0$ states. The corresponding one body density matrix (OBDM), the Fourier transform of $n(\mathbf{k})$, is $n(\mathbf{r})=\int d\mathbf{k}e^{ik\cdot r}n(\mathbf{k})=n_0+(1-n_0)n^*(\mathbf{r})$. The impulse approximation (IA), $J_{IA}(y)$, to the observed $J(Q,y)$ is the projection of $n(\mathbf{k})$ along $\mathbf{Q}$,

$$J_{IA}(y) = n(y) = \int d\mathbf{k}n(\mathbf{k})\delta(y-k_Q). \tag{2}$$

The $n(y)$ is denoted the longitudinal momentum distribution. The OBDM corresponding to $n(y)$ is $n(\mathbf{r})$ for atomic displacements s along $\mathbf{Q}$, $\mathbf{r}=\hat{\mathbf{Q}}s$,

$$n(s) = n_0 + (1-n_0)n^*(s). \tag{3}$$

A suitable model for $n^*(s)$ is a Gaussian plus possible higher order corrections

$$n^*(s) = \exp\left[-\frac{\bar{\alpha}_2 s^2}{2!} + \frac{\bar{\alpha}_4 s^4}{4!} - \frac{\bar{\alpha}_6 s^6}{6!}\right], \tag{4}$$

where the $\bar{\alpha}_n$ are adjustable fitting parameters. The observed $J(Q,y)$ can be expressed as a convolution of $J_{IA}(y)$ with the final state broadening fraction, $R(Q,y)$. We use the $R(Q,y)$ determined from measurements[34] in liquid ^{4}He as used previously in the solid.[35]

The OBDM Eq. (3), the Fourier transform of $J_{IA}(y)=n(y)$, is our basic model function. For a 3D bulk system where there is BEC, n_0 is a constant. There is "off diagonal long range order" (ODLRO) of magnitude n_0. In 2D, although superfluidity is not a consequence of BEC,[29] the onset of superfluidity is associated with the onset of algebraically decaying ODLRO.[30,31] That is, below T_c $n_0(s)$ is a slowly decaying function of s over $s \simeq 100$ Å. In either case, we can observe this order since we observe $n(s)$ out to lengths $s \simeq 6-7$ Å, only at the present Q values investigated. An n_0 is observed as a peaking in $J_{IA}(y)$ near $y=0$ as in trapped BEC systems.

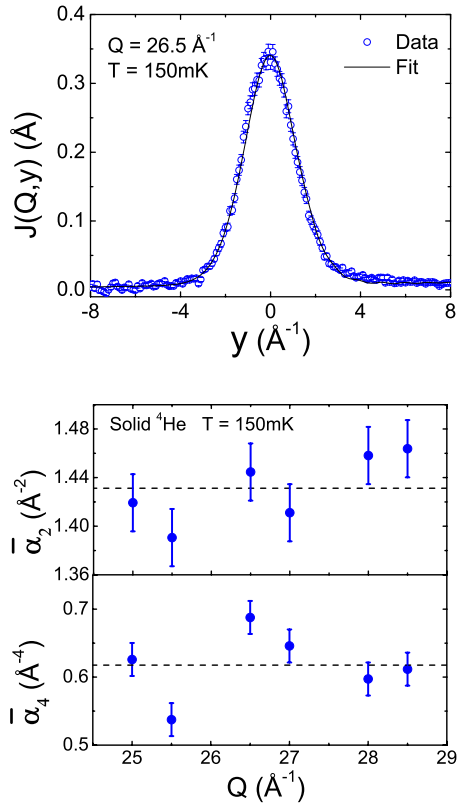

FIG. 2. (Color online) Upper: observed dynamic structure factor, $J(Q,y)$, at constant wave-vector transfer $Q=26.5$ $Å^{-1}$ versus energy transfer expressed in the wave-vector variable, y. The line is a fit of the model one body density matrix (OBDM) [Eq. (3)] to data with the condensate fraction set to zero. A good fit is possible. Lower: best fit values of $\bar{\alpha}_2$ and $\bar{\alpha}_4$ in Eq. (4) versus Q obtained from fits such as shown at $Q=26.5$ $Å^{-1}$.

Figure 2 shows the observed $J(Q,y)$ at $Q=26.5$ $Å^{-1}$ and temperature 150 mK. The solid line is a fit of the model OBDM [Eq. (3)] with $n_0=0$. The $\bar{\alpha}_2$ and $\bar{\alpha}_4$ in $n^*(s)$ are adjustable parameters. Only two parameters could be determined reliably in a fit so we neglected the higher order s^6 term. [We actually choose $\bar{\alpha}_6$ to have a small positive value, $\bar{\alpha}_6=0.02$ $Å^{-6}$, to ensure convergence of $n^*(s)$ at large s. Values of $\bar{\alpha}_6$ up to 0.3 $Å^{-6}$ can be used without significantly affecting the fitted values of $\bar{\alpha}_2$ and $\bar{\alpha}_4$]. Figure 2 also shows the best fit values of $\bar{\alpha}_2$ and $\bar{\alpha}_4$ obtained from similar fits at six Q values.

Clearly, the OBDM $n^*(s)$ in Eq. (3) with $n_0=0$ provides a good fit to the data at 150 mK in Fig. 2. Indeed, we found excellent fits to the data with $n_0=0$ at all three temperatures, 500, 150, and 65 mK. The data showed little dependence on temperature. To illustrate this, Fig. 3 shows the observed $J(Q,y)$ at 500, 150, and 65 mK at $Q=28.0$ $Å^{-1}$. The solid line is a fit of $n^*(s)$ (with $n_0=0$) to the data at 500 mK. The same $n^*(s)$ is simply superimposed on the data at 150 and 65 mK to show in a model independent way that the data at the

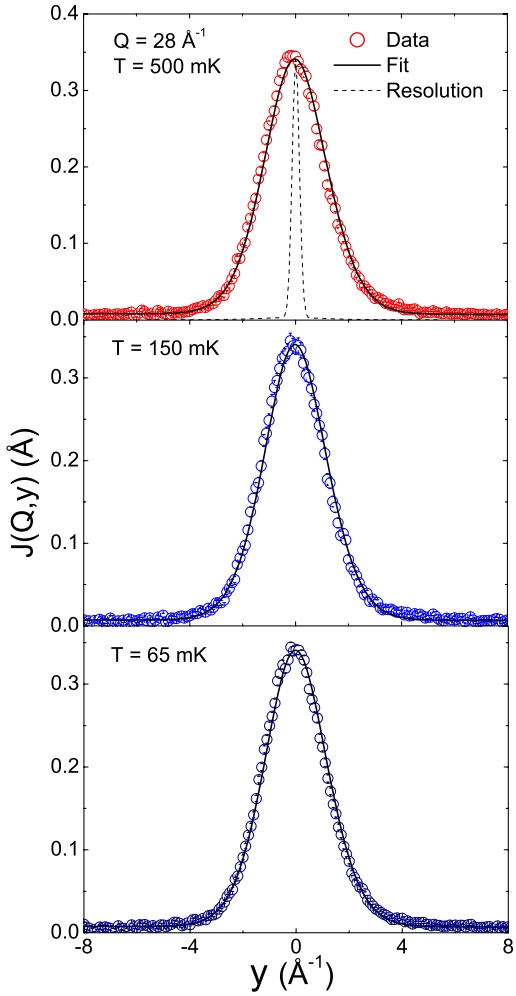

FIG. 3. (Color online) Observed $J(Q,y)$ at $Q=28.0$ Å^{-1} versus y at temperatures 500, 150, and 65 mK (circles). The solid line is a fit of the model OBDM with $n_0=0$ to the data at $T=500$ mK. The fit at 500 mK is superimposed on the data at 150 and 65 mK to show that the data are similar at each temperature. The dashed line is the instrument resolution.

three temperatures are similar. At 150 and 65 mK, there is no need to include a condensate to fit the data well. There is no peaking of $J(Q,y)$ at $y\simeq 0$ or other change in shape of $n(s)$ at 65 mK.

To quantify the temperature dependence, we note that the atomic kinetic energy (KE) is given by the width of the Gaussian component of $n^*(s)$ as $\mathrm{KE}=(3/2)\lambda\bar{\alpha}_2$ where $\lambda=\hbar^2/m=1.0443$ meV Å^2=12.12 K Å^2. With n_0 set to zero, values of $\bar{\alpha}_2$ at each temperature, averaged over Q, were obtained from fits to data. The average value of $\bar{\alpha}_2$ at 150 mK is shown as a dashed line in Fig. 2. The KE at 500, 150, and 65 mK are shown in Fig. 4. The KE clearly changes little with temperature.

At 500 mK, where $T\geq T_c$ and we expect $n_0=0$, the present $\mathrm{KE}=26.3\pm0.1$ K agrees well with previous high temperature values, for example, with $\mathrm{KE}=26.0\pm1.1$ K observed at $V_m=20.01$ cm^3/mol and $T=500$ mK and $\mathrm{KE}=24.25\pm0.30$ K observed at $V_m=20.87$ cm^3/mol and 1.6 K. We expect a somewhat larger KE in the present solid,

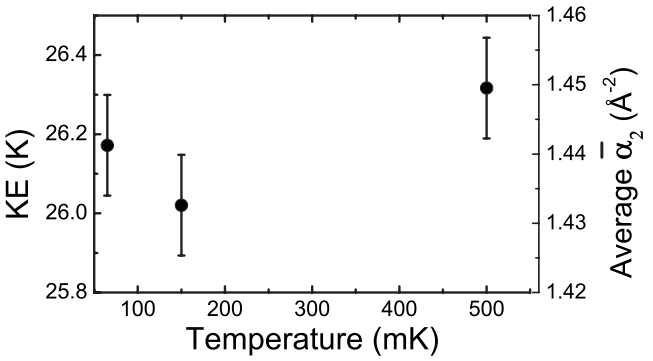

FIG. 4. The fitted parameter $\bar{\alpha}_2=\langle k_Q^2\rangle$ and the atomic kinetic energy, $\mathrm{KE}=(3/2)\lambda\bar{\alpha}_2$, where $\lambda=\hbar^2/m=1.0443$ meV Å^2 =12.12 K Å^2 versus temperature. The $\bar{\alpha}_2$ shown are the averages of $\bar{\alpha}_2$ over six Q values at each temperature.

which has a somewhat smaller volume ($V_m=19.8$ cm^3/mol). The $\bar{\alpha}_4$ values are independent of temperature within precision. They give a kurtosis of $n^*(\mathbf{k})$ of $\delta=\bar{\alpha}_4/\bar{\alpha}_2^2=0.3\pm0.1$, which is again consistent with previous experiments ($\delta=0.4\pm0.1$).[35]

To put bounds on n_0, we note again that at 500 mK, the observed $n(\mathbf{k})=n^*(\mathbf{k})$ is the momentum distribution for normal state vibration of the atoms about their lattice points. If superflow arises from BEC in surfaces or in glassy regions, we expect the $n^*(\mathbf{k})$ of the majority of the atoms in the bulk of the lattice to be largely unaffected by the appearance of BEC. To estimate n_0 in this picture we hold $n^*(\mathbf{k})$ fixed at its 500 mK value (i.e., $\bar{\alpha}_2$ and $\bar{\alpha}_4$ at their average values at 500 mK) and adjust n_0 to get a best fit at 150 and 65 mK. This yields the values of n_0 shown in Fig. 5. The average n_0 over six Q values is $n_0=0.0\pm0.3\%$ at 65 mK. Holding $n^*(\mathbf{k})$ fixed overestimates n_0 in liquid ^{4}He.

Alternatively, we could assume that $n^*(\mathbf{k})$ is affected by

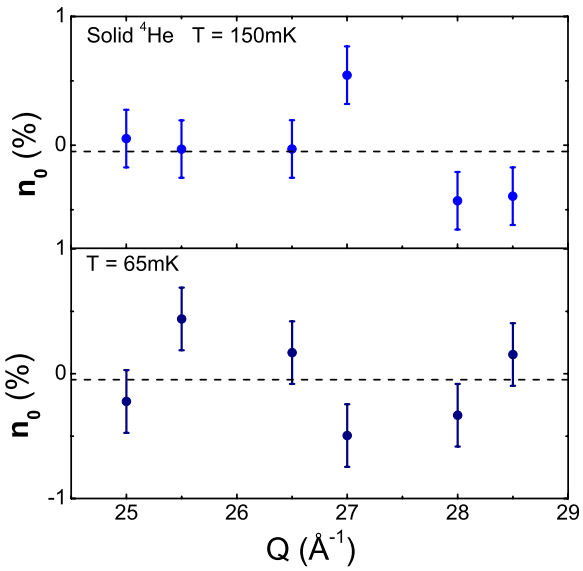

FIG. 5. (Color online) The condensate fraction n_0 versus Q at 150 and 65 mK obtained from fits to data with momentum distribution $n^*(\mathbf{k})$ for k values above the condensate held at its 500 mK value. The mean n_0 is $n_0=0.0\pm0.3\%$.

the onset of BEC, e.g., that the width $\bar{\alpha}_2$ as well as n_0 could change below T_c. In this case, we again find an average value of $n_0=0$ at $T=65$ mK and $T=150$ mK but with a marginally larger error bar reflecting the fact that two parameters are being adjusted (n_0 and $\bar{\alpha}_2$).

Recently, Hunt *et al.*[36] reported fascinating glassy behavior and significant relaxation times in the TO data of solid helium. The relaxation time to steady state is typically an hour at 50 mK. In the present experiment, neutrons were collected for 12 h at each temperature (24 h at 65 mK) and stored in 2 h batches. No change in the data with batch was detected indicating that neutron data from a solid in equilibrium was collected. Hunt *et al.*[36] also found an NCRI that saturates to its maximum value of 4.8% for $S/V=200$ cm^{-1} at 20 mK rather than at 50 mK.

In summary, our goal was to observe BEC in solid helium samples which have a large surface to volume (S/V) ratio. Large superfluid fractions have been reported in samples that have a large S/V, e.g., $\rho_S/\rho=20\%$ where $(S/V)\simeq 150$ cm^{-1}. Within precision, we observe no change in the shape of the atomic momentum distribution above and below $T_c \simeq 200$ mK in a sample for which $S/V=40$ cm^{-1}. This translates to a BE condensate fraction of zero within 0.3% at $T=65$ mK. This negative result suggests that either n_0 is small even where ρ_S/ρ is significant or the large ρ_S/ρ may be associated with rapid initial cooling rather than large S/V.[18] Sample quenching and a lower temperature[37] or increased precision may be required to observe BEC.

We thank Richard Down for valuable technical assistance at ISIS. This work was supported by the U.S. DOE, Office of Science (Grant No. DE-FG02-03ER46038).

[1] E. Kim and M. H. W. Chan, Nature (London) **427**, 225 (2004).
[2] E. Kim and M. H. W. Chan, Science **305**, 1941 (2004).
[3] Ann Sophie C. Rittner and J. D. Reppy, Phys. Rev. Lett. **97**, 165301 (2006).
[4] M. Kondo, S. Takada, Y. Shibayama, and K. Shirahama, J. Low Temp. Phys. **148**, 695 (2007).
[5] Y. Aoki, J. C. Graves, and H. Kojima, Phys. Rev. Lett. **99**, 015301 (2007).
[6] A. Penzev, Y. Yasuta, and M. Kubota, J. Low Temp. Phys. **148**, 677 (2007).
[7] A. C. Clark, J. T. West, and M. H. W. Chan, Phys. Rev. Lett. **99**, 135302 (2007).
[8] Ann Sophie C. Rittner and J. D. Reppy, Phys. Rev. Lett. **98**, 175302 (2007).
[9] E. Kim, J. S. Xia, J. T. West, X. Lin, A. C. Clark, and M. H. W. Chan, Phys. Rev. Lett. **100**, 065301 (2008).
[10] D. M. Ceperley and B. Bernu, Phys. Rev. Lett. **93**, 155303 (2004).
[11] M. Boninsegni, N. V. Prokof'ev, and B. V. Svistunov, Phys. Rev. E **74**, 036701 (2006).
[12] B. K. Clark and D. M. Ceperley, Phys. Rev. Lett. **96**, 105302 (2006).
[13] D. E. Galli, M. Rossi, and L. Reatto, Phys. Rev. B **71**, 140506(R) (2005).
[14] D. E. Galli and L. Reatto, J. Phys. Soc. Jpn. **77**, 111010 (2008).
[15] C. A. Burns, N. Mulders, L. Lurio, M. H. W. Chan, A. Said, C. N. Kodituwakku, and P. M. Platzman, Phys. Rev. B **78**, 224305 (2008).
[16] J. Bossy, J. V. Pearce, H. Schober, and H. R. Glyde, Phys. Rev. B **78**, 224507 (2008).
[17] Ann Sophie C. Rittner and J. D. Reppy, Phys. Rev. Lett. **101**, 155301 (2008).
[18] J. T. West, X. Lin, Z. G. Cheng, and M. H. W. Chan, Phys. Rev. Lett. **102**, 185302 (2009).
[19] J. Day and J. R. Beamish, Nature (London) **450**, 853 (2007).
[20] J. T. West, O. Syshchenko, J. R. Beamish, and M. H. W. Chan (unpublished).
[21] X. Lin, A. C. Clark, and M. H. W. Chan, Nature (London) **449**, 1025 (2007).
[22] X. Lin, A. C. Clark, Z. G. Cheng, and M. H. W. Chan, Phys. Rev. Lett. **102**, 125302 (2009).
[23] S. Sasaki, R. Ishiguro, F. Caupin, H. J. Maris, and S. Balibar, Science **313**, 1098 (2006).
[24] M. W. Ray and R. B. Hallock, Phys. Rev. Lett. **100**, 235301 (2008).
[25] S. Balibar and F. Caupin, J. Phys. Condens. Matter **20**, 173201 (2008).
[26] N. Prokof'ev, Adv. Phys. **56**, 381 (2007).
[27] O. Kirichek, arXiv:0810.5665 (unpublished).
[28] Nozières and D. Pines, *Theory of Quantum Liquids* (Addison-Wesley, Redwood City, CA, 1990), Vol. II.
[29] J. M. Kosterlitz and D. J. Thouless, J. Phys. C **6**, 1181 (1973).
[30] D. M. Ceperley and E. L. Pollock, Phys. Rev. B **39**, 2084 (1989).
[31] M. Boninsegni, N. Prokof'ev, and B. Svistunov, Phys. Rev. Lett. **96**, 105301 (2006).
[32] S. O. Diallo, J. V. Pearce, R. T. Azuah, J. W. Taylor, and H. R. Glyde, Phys. Rev. B **78**, 024512 (2008).
[33] S. O. Diallo, J. V. Pearce, R. T. Azuah, O. Kirichek, J. W. Taylor, and H. R. Glyde, Phys. Rev. Lett. **98**, 205301 (2007).
[34] H. R. Glyde, R. T. Azuah, and W. G. Stirling, Phys. Rev. B **62**, 14337 (2000).
[35] S. O. Diallo, J. V. Pearce, R. T. Azuah, and H. R. Glyde, Phys. Rev. Lett. **93**, 075301 (2004).
[36] B. Hunt, E. Pratt, V. Gadagkar, M. Yamashita, A. V. Balatsky, and J. C. Davis, Science **324**, 632 (2009).
[37] P. W. Anderson, Science **324**, 631 (2009).